


# Fractionation of Dissolved Organic Matter on Coupled Reversed-Phase Monolithic Columns and Characterisation Using Reversed-Phase Liquid Chromatography-High Resolution Mass Spectrometry

Sara Sandron<sup>1</sup> · Noel W. Davies<sup>2</sup> · Richard Wilson<sup>2</sup> · Alfonso Rojas Cardona<sup>1</sup> · Paul R. Haddad<sup>1</sup> · Pavel N. Nesterenko<sup>1</sup> · Brett Paull<sup>1</sup> 

Received: 29 January 2017 / Revised: 8 May 2017 / Accepted: 10 May 2017 / Published online: 25 May 2017  
© Springer-Verlag Berlin Heidelberg 2017

**Abstract** Eleven Onyx monolithic C<sub>18</sub> columns (100 x 3 mm) were connected in series to obtain a high-capacity reversed-phase HPLC column providing 110,000 theoretical plates. The column was used to fractionate a complex mixture of semi-polar and apolar components within marine dissolved organic matter (DOM), isolated using solid-phase extraction (SPE) on poly(styrene–divinylbenzene) cartridges, and Suwannee River natural organic matter, isolated by reverse osmosis. In each case, 15 isolated fractions were further separated using a second-dimension reversed-phase HPLC coupled with high-resolution mass spectrometry. Successful fractionation of the major compositional materials within DOM (i.e. carboxylic-rich alicyclic molecules, CRAM) in order of decreasing polarity was confirmed. Upon formulae assignment, homologous series of compounds were fractionated according to decreasing O/C ratio and increasing H/C ratio. Different compounds with the same exact masses were separated across six fractions, highlighting the immensely complex nature of the material, with the presence of potentially hundreds

of molecules for each molecular formula. Both samples showed clear compositional differences not only related to source (seawater or freshwater), but also to the extraction method applied (SPE or reverse osmosis).

**Keywords** Dissolved organic matter · Fractionation · Coupled monolithic columns · Reversed-phase liquid chromatography · High-resolution mass spectrometry

## Introduction

Dissolved organic matter (DOM) in seawater and freshwater represents a carbon reservoir comparable to atmospheric CO<sub>2</sub> (approx. 624 and 750 Gigatonnes, respectively) [1]. CO<sub>2</sub> is a primary product of DOM mineralisation, therefore an intimate link exists between this dissolved carbon pool and the atmosphere [1–3]. DOM contains various classes of compounds that are heterogeneous, polyfunctional, polyelectrolytic and polydisperse in molecular weight (typically between 300 and 7000 Da) and range in concentration from sub-picomolar to micromolar [4–6]. Composition varies considerably depending upon source, season and also depends on the extraction protocols applied [7, 8], with much of this material remaining uncharacterised, in particular the innumerable species present at trace levels.

The extraordinary complexity of DOM often precludes the use of many liquid chromatographic techniques due to insufficient resolution [9–11] and problems associated with widely varying retention factors of such diversity of material onto most types of stationary phases [12–14]. In the case of gas chromatography (GC), there can also be significant compositional and conformational changes due to chemical degradation and the use of derivatisation

Published in the topical collection *2nd ACROSS International Symposium on Advances in Separation Science (ASASS 2016)* with guest editors Pavel Nesterenko and Brett Paull.

**Electronic supplementary material** The online version of this article (doi:10.1007/s10337-017-3324-0) contains supplementary material, which is available to authorized users.

✉ Brett Paull  
brett.paull@utas.edu.au

<sup>1</sup> Australian Centre for Research on Separation Sciences, School of Physical Sciences, University of Tasmania, Sandy Bay, Hobart 7001, Australia

<sup>2</sup> Central Science Laboratory, University of Tasmania, Sandy Bay, Hobart 7001, Australia

procedures, causing a subsequent loss of sample integrity, particularly for sensitive non-refractory material [9, 10, 15]. Reversed-phase HPLC has been applied for the partial separation of DOM, in particular for the stable and non-volatile fraction, which includes carboxylic-rich alicyclic molecules (CRAM), molecules derived from linear terpenoids (MDLT), lignin derivatives, peptides and carbohydrates [16–18]. However, inadequate resolution necessitates the use of hyphenated approaches including information-rich detectors, such as high-resolution mass spectrometry (HRMS) and multidimensional NMR, to provide insight into the nature of unresolved material and further the molecular characterisation of DOM [19–23].

Even with the considerable combined separation capacity of hyphenated techniques such as HPLC-HRMS, the identification and isolation of unique structures within DOM still presents a significant challenge, due to the limited capacity and chromatographic resolution achievable [23–26]. Chromatographic methods with increased capacity and separating power are required, including multidimensional chromatographic approaches, with the capacity to fractionate sufficient quantities of DOM, as required to provide sufficiently concentrated fractions for further separation and characterisation [14, 27–32].

In the present study, a new chromatographic approach is presented for the prefractionation and subsequent RP-HPLC-HRMS characterisation of DOM from both marine and freshwater sources, based upon the use of a high (loading) capacity and high efficiency monolithic RP-HPLC column, composed of eleven columns (total dimensions-110 cm x 3mm) coupled in series [33]. This long monolithic column provided for the collection of 15 fractions from each DOM sample, each being subjected to further separation and characterisation using RP-HPLC-HRMS. This approach confirmed the presence and distribution of major classes of material, such as CRAM, highlighting both general fractional characteristics, such as average size and polarity, and more specific compositional information, such as H/C ratio and O/C ratio, each acting to confirm successful fractionation. The results presented herein, obtained using this novel off-line multidimensional chromatographic approach, provide a dramatic illustration of the nature and overall complexity of DOM.

## Materials and Methods

### Chemicals, Standards and Reagents

Methanol (MeOH) and formic acid (HPLC and MS grade) were purchased from Sigma Aldrich (Sigma Aldrich, Sydney, Australia). Deionised (DI) water was obtained from a Milli-Q water purification system (Millipore, Watford,

UK). Nitric acid, sodium chloride and hydrochloric acid, used for preparation of washing solutions, artificial seawater and seawater acidification, respectively, were also obtained from Sigma Aldrich (Sigma Aldrich, Sydney, Australia). Suwannee River natural organic matter (NOM) reference material was purchased in dry form from the Humic Substances Society (Humic Substances Society, IHSS, Denver, CO, USA), having been extracted using reverse osmosis as described by Serkiz et al. and Sun et al. [34–36].

### Seawater Collection and DOM Extraction

Coastal seawater samples (25 L volumes) were collected from the Tasman Peninsula (Koonya, Tasmania, 43.1000°S, 147.7500°E, March 2014), and briefly stored in polypropylene containers at 4 °C prior to extraction. The containers were prewashed with several volumes of 0.1 M HNO<sub>3</sub>, DI water, MeOH, acetone and DI water once more, before sampling. The DOM was isolated precisely as described by Dittmar et al. [37, 38]. The samples were filtered through Nucleopore (Agilent, Mulgrave, VIC, Australia) polycarbonate filter cartridges (3, 1 and 0.20 μm pore sizes, sequentially) and glass microfiber Whatman GF/F filters (0.70 μm pore size) (Agilent, Mulgrave, VIC, Australia). Samples were acidified using concentrated HCL to pH 2 to improve recovery of organic and phenolic acids during subsequent SPE. The filtered water samples (25 L) were then gravity fed through Varian Bond Elut PPL cartridges, containing a non-polar surface modified styrene-divinylbenzene (S-DVB) sorbent (1 g, 60 mL) (Agilent, Mulgrave, VIC, Australia), with the retained DOM eluted using one cartridge volume of MeOH, and subsequently concentrated by rotary evaporation. The isolated DOM was stored in the dark at –20 °C, prior to chromatographic fractionation in order to preserve the sample from photochemical or microbial based degradation.

Artificial (blank) seawater was prepared and used to identify and exclude artefacts or contaminants from sample storage and extraction protocols being evident within later HRMS spectra. Briefly, a 25 L saline solution of 0.52 M analytical grade NaCl (≥99.5%), previously dried at 120 °C, was prepared, and treated, stored and extracted according to the procedure presented in Dittmar et al. [37].

### DOM Fractionation

Eleven Onyx monolithic reversed-phase (C<sub>18</sub>) columns (each 100 × 3.0 mm ID) were obtained from Phenomenex (Lane Cove West, NSW, Australia) and connected in series using minimum lengths of 0.254 mm ID PEEK tubing (see ESI Figure S1). This coupled monolithic column (CMC) was connected to an Agilent 1200 series HPLC

system, consisting of a pump, a degasser and an autosampler module (Agilent, Mulgrave, VIC, Australia). Sample injection volume was 10  $\mu\text{L}$  of 25 mg/mL DOM solutions (MeOH/0.1% formic acid). A flow-rate of 0.27 mL/min was selected, based upon  $H_{\text{min}}$  determined from a Van Deemter plot produced for a single solute (anthracene) separated on the full 110 cm long CMC. For DOM fractionation, a simple water/MeOH linear gradient was applied, from 10 to 70% MeOH/0.1% formic acid over 360 min (details available within ESI Table S1). These CMC separations were carried out in triplicate, using UV absorbance detection at 210 nm with a Waters 486 UV detector (Milford, MA, USA), and specific sample fractions collected from each subsequent injection combined. Blank extracts from the artificial seawater were fractionated identically. Fractions were collected according to 30 min time intervals, with precise details being provided within ESI Table S2, and shown graphically within Fig. 1. Figure 1 shows the DOM chromatogram obtained following the electronic subtraction of the equivalent extracted artificial seawater blank sample.

### Reversed-Phase Liquid Chromatography-High Resolution Mass Spectrometry

The fractions were collected in triplicate from the CMC, combined, and reduced in volume under nitrogen, and recovered in 150  $\mu\text{L}$  in MeOH/0.1% formic acid, for further separation using a Waters Alliance 2690 separation module (Milford, MA, USA). A 30  $\mu\text{L}$  aliquot of each sample was injected onto a Waters Nova-Pak  $\text{C}_{18}$  column, 150  $\times$  4.0 mm ID, particle size 4  $\mu\text{m}$ ) at a flow rate of

0.8 mL/min. MS-grade solvents (0.1% formic acid in water and 0.1% formic acid in MeOH) were employed during a 30 min linear gradient of 10–100% MeOH. The column was operated at ambient temperature (20  $^{\circ}\text{C}$ ) and coupled to a hybrid Linear Trap Quadrupole/Orbitrap (Thermo Fisher Scientific, Bremen, Germany) mass spectrometer, for HRMS characterisation. Centroid mass spectra were acquired over the range  $m/z$  50–1000 at a target resolution of 30,000, operating using the following parameters: capillary temperature of 300  $^{\circ}\text{C}$ ; sheath gas and auxiliary gas flow rates were set to 30 and 5 au (arbitrary units), respectively. A capillary voltage of 7 V was used for negative ion acquisition.

From the RP-HPLC-HRMS total ion current (TIC) chromatograms obtained for the fifteen fractions collected for each sample, averaged mass spectra were obtained from the retained peaks of interest. From these averaged spectra, molecular formulae were assigned using Xcalibur molecular formulae calculator (Thermo Fisher Scientific, Bremen, Germany). The following parameters were used: All detected ions were singly charged, as determined by the unit  $m/z$ , mass tolerance 2 ppm, 50 as maximum number of carbons, 100 as maximum number of hydrogens and 30 as maximum number of oxygens, and a S/N ratio  $>20$ . In this study, other elements such as nitrogen, sulfur and phosphorus were not considered, in order to target the portion of DOM typically referred to as CRAM and CRAM-like material. Inconsistent formulae assignments or those not obeying the nitrogen rule were ruled out together with  $m/z$  reporting a relative signal intensity lower than 5%. Each fraction spectrum showed on average  $\sim 3000$  peaks at S/N

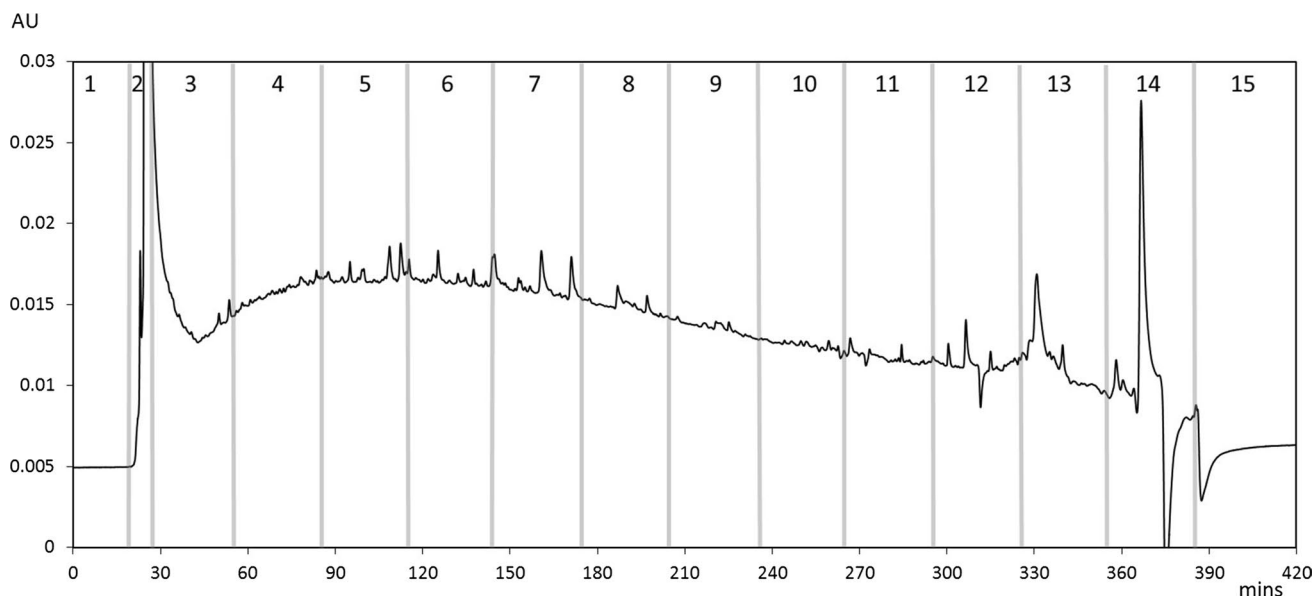


**Fig. 1** RP-HPLC–UV fractionation of coastal seawater DOM. Column: coupled Onyx monolithic  $\text{C}_{18}$  columns (11  $\times$  100  $\times$  3.0 mm). Flow rate = 0.27 mL/min. Gradient: 10–70% MeOH/0.1% formic acid over 360 min

>20. Of these, 2200 (~75%) were assigned with a molecular formula after complying with the limiting parameters.

## Results and Discussion

### DOM Fractionation

As seen with previous chromatographic approaches to DOM fractionation [12, 22, 39, 40], the complexity and diverse range of material present, results in a typically broad and poorly resolved chromatogram, best described as an ‘unresolved hump’ or ‘hump-a-gram’. This is particularly the case with past studies based upon the use of standard (in both capacity and efficiency) reversed-phase columns for DOM fractionation [19]. Herein, in an attempt to improve upon the degree of DOM fractionation achieved, whilst simultaneously increasing the mass of DOM which could be fractionated per injection, a 110 cm × 3 mm coupled reversed-phase monolithic column was applied. The maximum sample mass that can be loaded is dependent upon both the length and diameter of the column [41]. For standard bore columns, increasing column length provides capacity for increased sample loading, particularly when gradient elution is applied, which provides band compression. Monolithic columns, with their relatively low column back pressures allow multiple columns to be coupled, without requiring ultra-high pressure pumps. The use of the CMC provides both a high separation efficiency ( $N > 100k$ ) and sufficient sample loading capacity, both crucial in the fractionation of a complex mixture such as DOM. Additionally, the coupled column format allowed decoupling, washing and if necessary replacement of the leading monolith, should evidence of column irreversible fouling appear (common when dealing with DOM). Herein, the goal was to provide the desired fractionation of the DOM within the broadly eluting ‘hump’. The application of a simply shallow linear gradient provided just such an elution profile, with continuous elution of material over the entire

applied gradient, with the unretained highly polar compounds (e.g. amino acids, sugars and small organic acids) marking the void time at 23 min. Figure 1 shows the full RP-HPLC–UV (210 nm) chromatogram obtained for the coastal DOM sample on the CMC, with the 15 fractions collected highlighted. In the chromatogram shown the baseline from the applied solvent gradient has been subtracted, to clearly show the full breath of the eluting material over the period 20–290 min, with the last eluting fractions presumably representing the most non-polar bulky materials (the long fractionation time could be reduced through increased flow rate given the low column pressure drop for the CMC relative to length, however here the fractionation time was not a priority parameter). A very similar profile was obtained for the sample of Suwannee River NOM reference material.

Based upon previous reversed-phase separations of DOM, it is reasonable to assume that the majority of the intermediate polarity material would begin to be eluted beyond 60 min (mobile phase ~50% MeOH 0.1% formic acid and 50% water 0.1% formic acid), which would include the bulk of that classified as CRAM and CRAM-like material. As discussed by Hertkorn et al., CRAM molecules are characterised by condensed aliphatic rings with a varying degree of carboxylation and unsaturation, which result in these compounds displaying an intermediate degree of polarity [16]. With RP-HPLC, highly carboxylated CRAM molecules would be expected to be eluted earlier, with less carboxylated counterparts showing greater retention [14]. However, to date the chromatographic separation of CRAM itself with any significant degree of resolution has not been demonstrated. Typical CRAM structural isomers, elucidated by means of both HRMS and NMR by Hertkorn et al. [16] can be seen in Fig. 2, where three isomers with formula  $C_{28}H_{32}O_{13}$  are presented. Within these series of molecules of same nominal mass, sequential mass differences of 36.4 mDa (the difference between O and  $CH_4$ ) are observed, as well as series differing by 2.0157 Da, reflecting a difference of 2H [16].

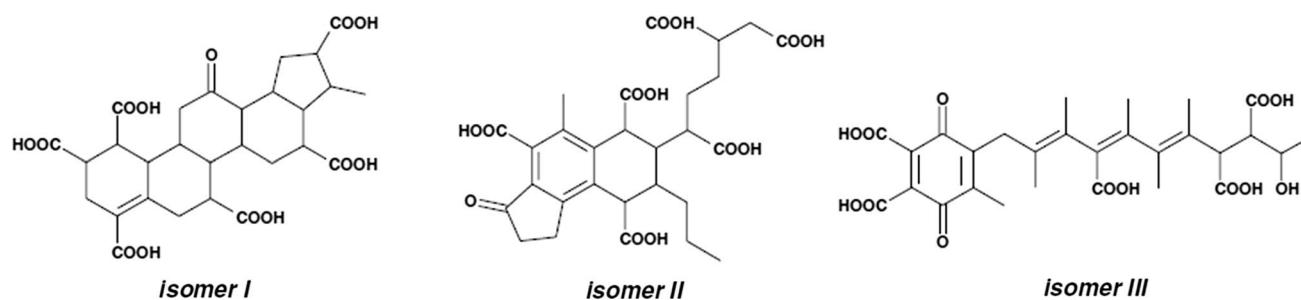


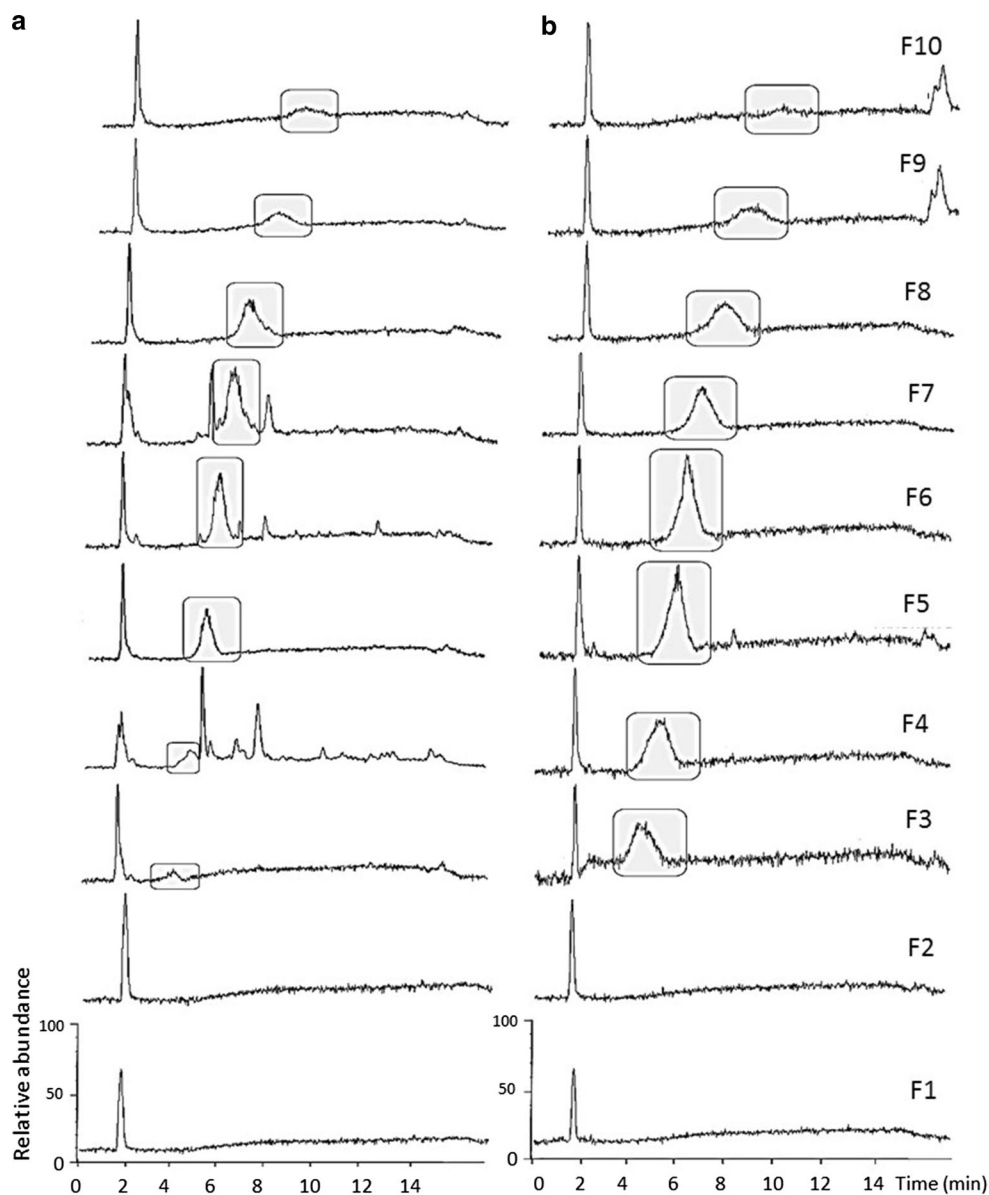
**Fig. 2** Molecular structures for three  $C_{28}H_{32}O_{13}$  isomers. Image obtained from Hertkorn et al., with permission [16]

### Fractional Analysis: RP-HPLC-HRMS

Figure 3a, b shows the RP-HPLC-HRMS TIC chromatograms obtained for a number of the individual fractions collected from the CMC separation for both the (a) coastal seawater DOM sample and the (b) Suwannee River NOM reference material. Both samples (10  $\mu$ L inj. vol.) were injected onto the CMC at a solution concentration of 25 mg/mL, collected, concentrated and reconstituted equally. The use of RP-HPLC as a second chromatographic separation immediately reveals the success of the fractionation approach and produces a series of TIC chromatograms showing very clear similarities between the two samples. Here, the typical unresolved DOM 'hump' has been replaced with a series of relatively Gaussian shaped peaks, which appear from ~fraction 3 and increase

in retention sequentially until ~fraction 10 (most clearly seen with the Suwannee River sample), and both showing maximum intensity around fractions 6 to 7. Although clearly still a cluster of co-eluted material, these peaks are eluted in a relatively narrow elution window and demonstrate a very obvious correlation between fraction number (retention on reversed-phase CMC) and retention on this second reversed-phase column. This is particularly evident with the Suwannee River NOM results, where the fractions are remarkably clear of other eluted material, besides this increasingly retained broad peak. In the case of the coastal seawater sample, the TIC chromatograms display an overall lower concentration of this common composite peak. A plot of fractionation time (mid-point of the fraction window) against retention time for the highlighted composite peaks in the second dimension chromatograms

**Fig. 3** RP-HPLC-HRMS TIC chromatograms for fractions 1–10 (collected in triplicate, combined and reconstituted) for both **a** coastal seawater DOM and **b** Suwannee River NOM through. Column: Waters Nova-Pak C<sub>18</sub> (150  $\times$  3.9 mm ID), flow rate 0.800 mL/min of a 10–100% MeOH 0.1% formic acid in water 0.1% formic acid gradient in 25 min



gave two linear plots ( $R^2 = 0.975$  for coastal seawater and  $R^2 = 0.962$  for Suwannee River), with both samples displaying very similar slopes, as expected with the separation mode being reversed-phase in both cases, and so no significantly selective orthogonality is evident (the use of similar phases in first and second dimensional LC analysis is not uncommon, particularly when the aim is to fractionate to reduce sample complexity for second dimension LC-MS analysis. Herein, the goal was not to generate complex 2D chromatographic profiles wherein column orthogonal selectivity would be more beneficial). To clearly demonstrate the fractionation achieved, a sample containing unfractionated coastal seawater DOM was analysed directly with the RP-HPLC-HRMS system, with the resultant TIC chromatogram shown as Fig. 4. Here the broad unresolved materials (typical DOM 'hump-a-gram') were eluted over the period from 4 to 12 min.

The highlighted composite peaks within Fig. 3 demonstrate slight evidence of fronting, which could reflect some column overloading due to the complexity of the material (even following fractionation), or the equilibria of multiple species present within each peak [42]. With reversed-phase selectivity it was expected that more polar materials, i.e. compounds richer in carboxyl functional groups and double bonds, should be evident within the earlier fractions, compared to that present within the later fractions. To investigate the nature of each of the fractional peaks, an intensity versus  $m/z$  plot was produced for each fraction from both samples, containing all species present over the minimum intensity threshold. A selection of these plots is presented as Fig. 5.

The data show a number of significant compositional differences between the two sets of fractions. In the case of the Suwannee River sample fractions, there appears to be a much greater diversity of material, with a dense population of low intensity (albeit above the set threshold) signals spanning the 100–700  $m/z$  range. There also appears to be densely populated regions between  $m/z$  100 to ~360 (all below int. 2000), most obvious within fractions 5–7 of the seawater sample, but also seen within fractions 7–9 of the Suwannee River material, which act to skew the otherwise normal distributions.

In the intensity versus  $m/z$  distributions for both samples, a gradual shift towards higher molecular weights could be observed from the early to later eluted fractions. However, to visualise this more clearly, the weighted means ( $\bar{x}_w$ ) of the  $m/z$  distributions for each composite peak in each fraction (3–10) from both samples were calculated and then plotted against the retention time for the associated composite peak. These plots are shown as Fig. 6a, and confirm a number of points. Firstly, both samples show a correlation between their weighted average  $m/z$  values and retention time, with  $R^2 = 0.983$  for the coastal seawater

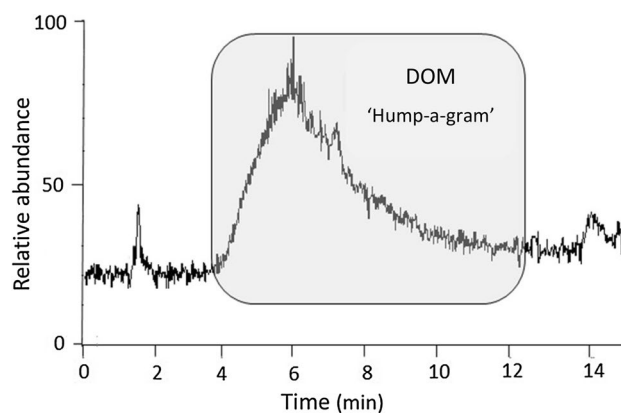


**Fig. 4** RP-HPLC-HRMS chromatogram obtained for the unfractionated coastal seawater DOM sample. Column: Waters Nova-Pak C<sub>18</sub> (150 × 3.9 mm ID), flow rate 0.800 mL/min of a 10–100% MeOH 0.1% formic acid in water 0.1% formic acid gradient in 25 min

sample, and 0.990 for the Suwannee River reference material. For example, for the coastal seawater DOM sample, the weighted mean was equal to  $m/z$  360 for the composite peak within fraction 3,  $m/z$  373 for fraction 5,  $m/z$  383 for fraction 7, and  $m/z$  405 for fraction 9. Similarly, regular increases in weighted average  $m/z$  values are seen with the Suwannee River sample ( $m/z$  354 for fraction 3,  $m/z$  381 for fraction 5,  $m/z$  393 for fraction 7, and  $m/z$  417 for fraction 9), thus confirming in both instances the success of the fractionation process. Figure 6b, c shows the full data set for each sample, further illustrating this selectivity.

Secondly, the plots clearly reveal differences in the retention times for the composite peaks within each respective sample fraction, which obviously reflects the compositional differences highlighted within the  $m/z$  distribution diagrams (Fig. 5). The overall nature of these compositional differences across the collected fractions is then revealed in the different slopes obtained within the above  $m/z$  vs retention plots (Fig. 6a). Of the two sets of data, the Suwannee River material exhibited the greater slope (SR = 15.31; SW = 12.43), together with the extended  $m/z$  range (weighted average  $m/z$  for SR F9 = 417; weighted average  $m/z$  for SW F9 = 405). This extended range is probably due to the reverse osmosis extraction process used to isolate the reference material, compared to the SPE-extracted seawater DOM sample. This observation would be consistent with results reported by Koprivnjak et al., and more recently by Tfiailly et al., which emphasised that organic matter recovered through reverse osmosis displayed a wider molecular weight distribution (200–1000 Da) compared to that obtained using alternative extraction techniques (i.e. ultrafiltration and SPE) [43–46]. The differing slopes reveal that the compositional differences in the two samples are such that at the lower  $m/z$  range, greater retention is seen for the Suwannee River material, with this relative difference

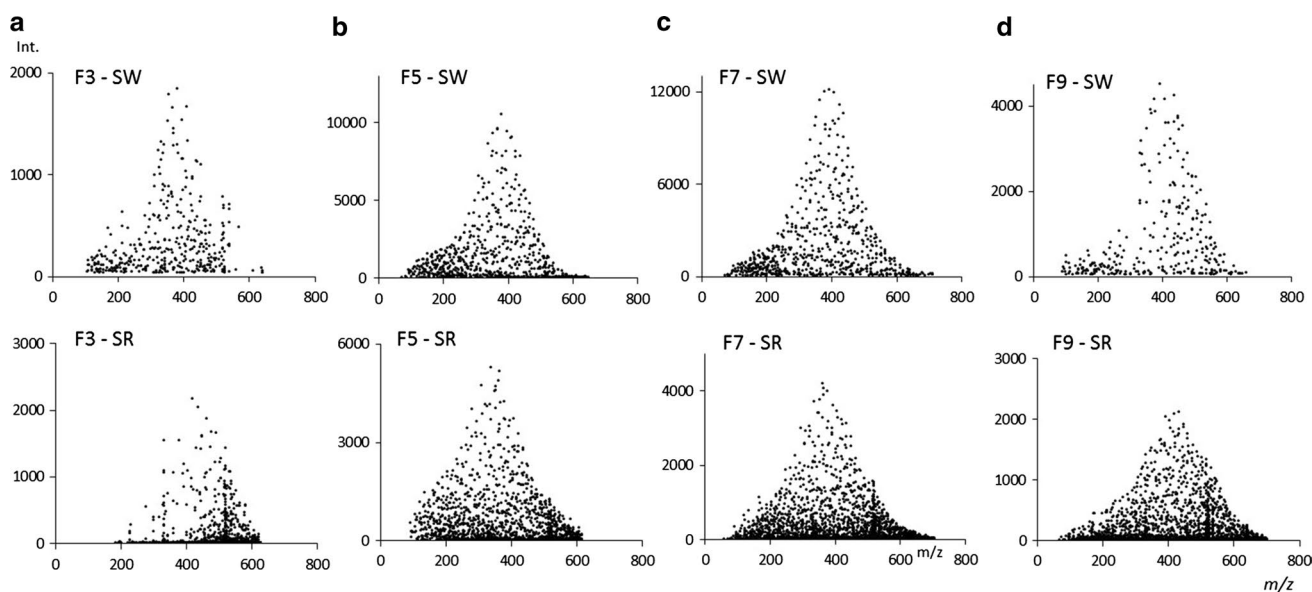


**Fig. 5** Intensity versus  $m/z$  distribution of the compounds eluting within four representative CRAM-containing fractions from TICs represented in Fig. 3: **a** fraction 3, **b** fraction 5, **c** fraction 7 and **d** fraction 9 for Koonya seawater DOM (*top*) and Suwannee River NOM (*bottom*)

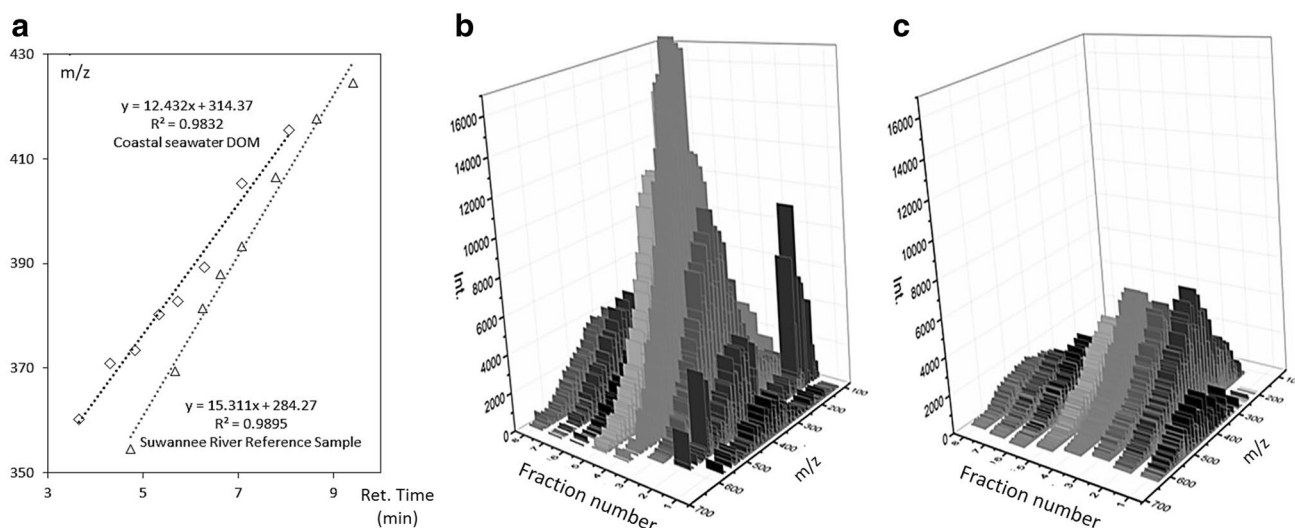


**Fig. 6** **a** Plots of weighted average  $m/z$  versus retention time for the composite peaks isolated within fractions from the coastal seawater DOM and Suwannee River NOM. **b** 3D plots showing  $m/z$  distribu-

tion, intensity and fraction number for the isolated composite peaks obtained from the Suwannee River NOM and samples **c** coastal seawater DOM

decreasing with increasing  $m/z$ . Indeed, were the regression lines extrapolated further to higher  $m/z$  values, the slopes would reveal a reversal of this effect at  $\sim 445$   $m/z$ , where the composite peaks from the seawater DOM would show greater retention.

The observed differences in relative retention are likely to reflect differences in degrees of saturation and oxidation, as might well be expected for two samples of differing origin (and extraction procedures). Therefore, the datasets were further examined with regard to specific H/C and O/C ratios.

For each C, H and O containing compound with an assigned formula, H/C and O/C ratios were calculated. These data were used to further elucidate the observed selectivity during fractionation based upon molecular characteristics.

As expected the above formulae assignments revealed extensive fraction-to-fraction occurrences of the same molecular formulae; however, significant patterns could be identified. The data are presented here as Van Krevelen diagrams (Fig. 7), for coastal seawater DOM and Suwannee River fractions 3, 5, 7 and 9, and also as the O/C ratio

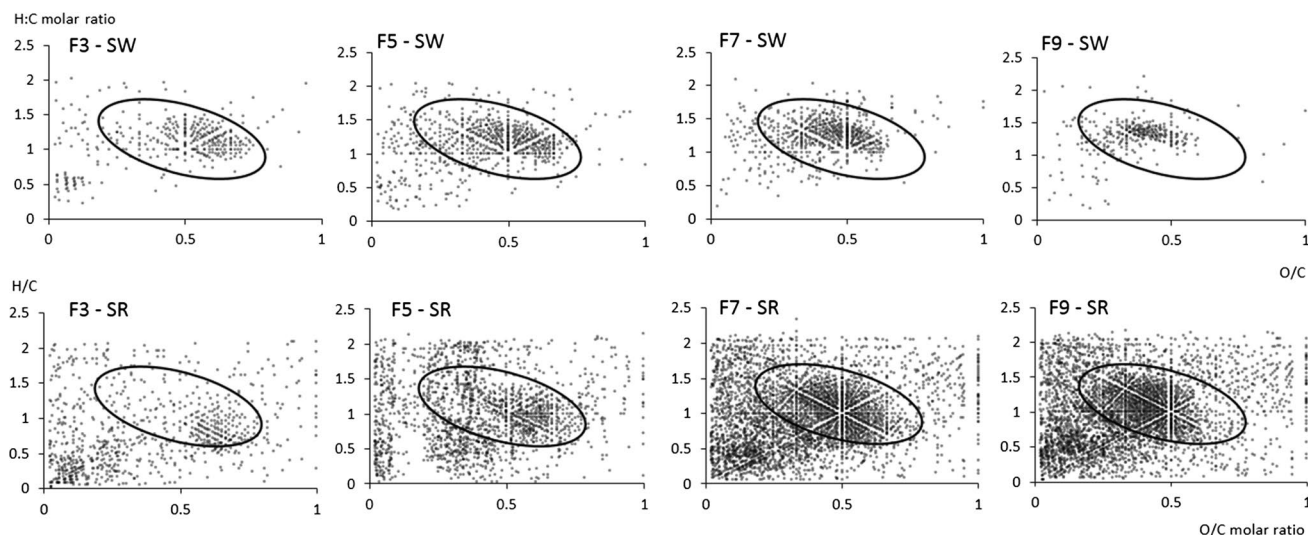


**Fig. 7** Van Krevelen diagram of H/C versus O/C for the compounds eluting within four representative CRAM-containing fractions from TICs represented in Fig. 2: fraction 3, fraction 5, fraction 7 and frac-

tion 9 for coastal seawater DOM (SW) (*top*) and Suwannee River NOM (SR) (*bottom*). Typical CRAM and CRAM-like materials region highlighted [46]

versus  $m/z$  for all of the same four fractions (Fig. 8). Molecules are clustered according to their functional group composition, as every point represents each molecular formula assigned by mass spectra [46–48].

Taking the less complex coastal seawater DOM fractions, the Van Krevelen diagrams reveal that the bulk of the typical CRAM and CRAM-like materials (highlighted region within Fig. 7 [47]) are presenting between fractions 5 and 7. Materials of high O/C ratios above 0.7 are notably sparse (e.g. tannins, carbohydrates), and there is some evidence for the elution of the majority of the low O/C—low

H/C material between fractions 3 and 5. Somewhat similar elution behaviour can be seen with the Suwannee River material, although the highlighted region associated with CRAM and CRAM-like material extends further, being most evident within fractions 7–9. There is also clearly a far greater density of low O/C—low H/C ratio material, the majority of which is eluted within the later fractions. As already highlighted in previous studies, greater diversity and concentration of highly unsaturated compounds is usually observed in HRMS spectra from terrestrial and coastal marine samples [43]. The higher degree of unsaturation

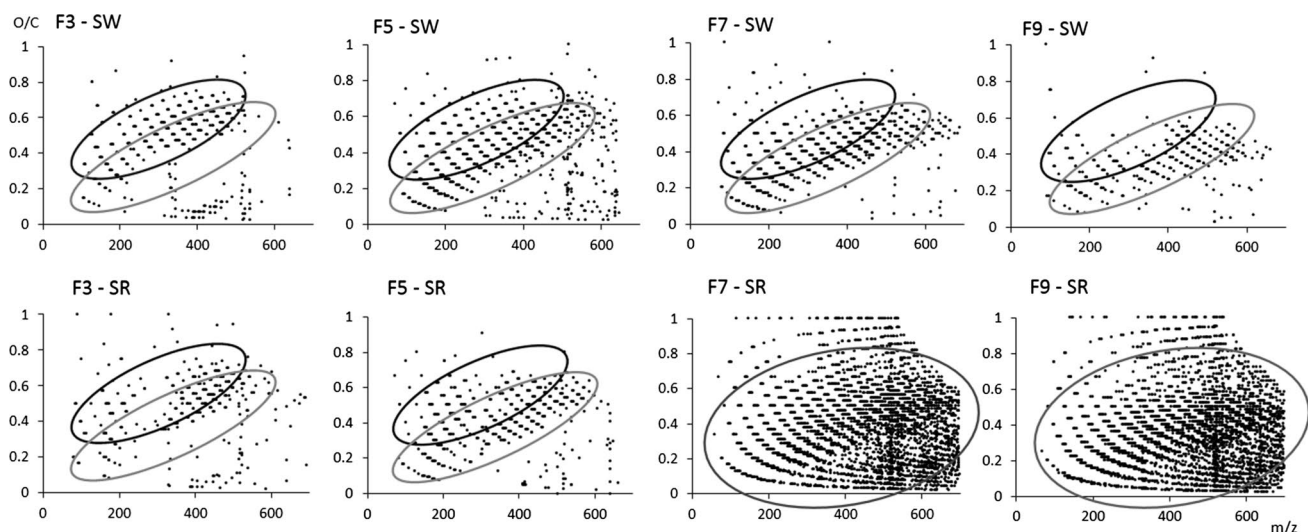


**Fig. 8** O/C versus  $m/z$  of homologous series from the compounds eluting within four representative CRAM-containing fractions from TICs represented in Fig. 2: fraction 3, fraction 5, fraction 7 and frac-

tion 9 for coastal seawater DOM (SW) (*top*) and Suwannee River NOM (SR) (*bottom*). Migration of densely populated regions (black into grey zones) is highlighted



for compounds extracted from freshwater samples is commonly due to their higher degree of aromaticity, which is typical of terrestrially derived and lignin-like materials [49]. This can be seen in Fig. 7, where Van Krevelen diagrams for the Suwannee River reference sample fractions are more heavily populated with compounds with  $H/C < 1.0$ , and  $O/C < 0.5$ . However, in a recent comparison of Van Krevelen plots for DOM obtained using either SPE or dialysis based methods, carried out by Tfaily et al., this low  $O/C$  region was shown to be notably more populated when the sample was isolated using dialysis, and so herein is also likely to be reflective of differences in DOM isolation technique [46].

Comparison of fractional plots presented within Fig. 8 reveals a common trend of decreasing  $O/C$  ratio and increasing  $m/z$ , with increasing retention. This is demonstrated most clearly with the coastal seawater fractions, where the migration of densely populated regions is highlighted (black into grey highlighted regions). Again a similar effect is seen for the Suwannee River fractions, albeit at a somewhat less obvious level due to the much higher density of high  $m/z$ , low  $O/C$  material present in the later eluted fractions. Figure 8 dramatically reveals the substantial number and extensive range of homologous series' in each sample. Within fractions 3–9, series' of molecules differing by one oxygen atom or one carbon atom and four hydrogen atoms can be seen, demonstrating a typical increase in oxidation with a decrease  $m/z$  (i.e. variation in methylene count). These differences, and assigned formulae, within one such homologous series are highlighted within the Electronic Supplementary Material as Figure S2. Further to this, other recurrent mass differences between the observed ions are defined by the variation in double

bond equivalents [16, 50, 51]. Typical series such as those shown have been described by Hertkorn et al. and defined as CRAM [16, 52]. In some instances series' are predominantly present in specific fractions, for example direct comparison of fractions 3 and 9 for the coastal seawater sample, confirming that CRAM was fractionated according to its degree of oxidation.

### Chromatographic Resolution

It should be noted here that each of the assigned formulae covers a large number of structurally diverse isomers. Thus the degree of complexity existing across the collected fractions is truly remarkable. To demonstrate the chromatographic resolution achieved herein, a number of relatively abundant masses were selected and the chromatographic retention/selectivity for peaks corresponding to those masses within each fraction was determined using RP-HPLC-HRMS. These single ion chromatograms for these fractions, within which each ion was evident, were highly illustrative of the underlying resolution achieved on the long monolithic column. Figure 9 shows these overlaid single ion chromatograms for two selected ions, namely  $m/z$  383.0985, ( $C_{17}H_{19}O_{10}$ ) and  $m/z$  505.1145 ( $C_{27}H_{21}O_{10}$ ), for each sample.

For  $m/z$  383.0985, ( $C_{17}H_{19}O_{10}$ ), Fig. 9 reveals the presence of peaks of this exact nominal mass eluted in fractions 3 through to 8 of the coastal seawater DOM, each showing increased (unique) retention on the second dimension reversed-phase column. Peak widths, compared to those expected for a single reference standard, would indicate that each peak within each fraction was a composite isomeric peak of material of very similar

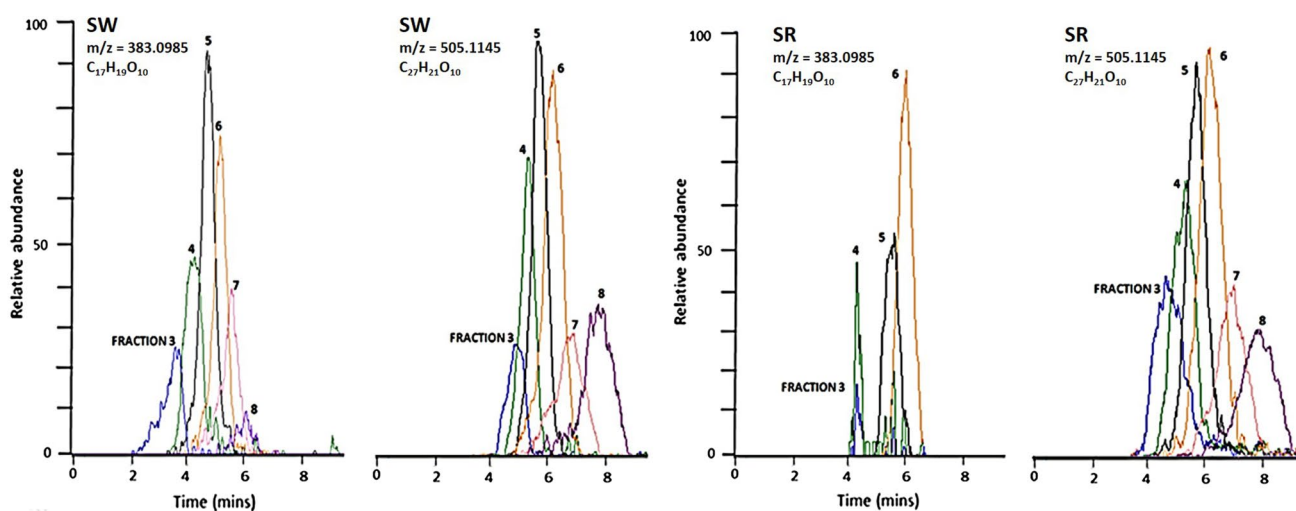


**Fig. 9** RP-HPLC-HRMS single ion chromatograms from the monolith column fractions for  $m/z$  383.0985  $\pm$  1 ppm for the formula  $C_{17}H_{19}O_{10}$ , and  $m/z$  505.1145  $\pm$  1 ppm for the formula  $C_{27}H_{21}O_{10}$ , in

coastal seawater DOM (SW) and Suwannee River NOM (SR). Data are normalised to the strongest signal in each case

reversed-phase selectivity. Therefore, the overlaid fractions contain potentially dozens of compounds with  $[M - H]^-$  ions at  $m/z$  383.0985, which given the resolution shown on this second dimension RP-HPLC separation (i.e. the composite isomeric peaks are not co-eluted across all the fractions), means these groups of isomers were indeed fractionated on the first dimension monolithic column.

For the Suwannee River reference material, the pattern for the same ion is very different, with the bulk of the material isolated within fractions 3–6. The efficiency (peak width) of the peak for fractions 3 and 4 for Suwannee River NOM, confirm the composite nature of the other broader peaks, and indicate a much smaller isomeric diversity within these two fractions. Interestingly, there is no resolution observed for this particular smaller cluster of isomers on the first dimension separation (data not shown), which would indicate these collectively eluted at the boundary point of the two fraction collection zones.

Taking the ion  $m/z$  505.1145, ( $C_{27}H_{21}O_{10}$ ) as a second example (Fig. 9), more similarities can be seen between the two samples. For both coastal seawater DOM and Suwannee River NOM, the ion is evident from fraction 3 through to 8, with reasonable resolution of each isomeric composite peak provided during fractionation. The retention time correlation between the two sets of sample fractions was also interesting to note (taking peak maximum of each composite fraction peak), with fraction 3 retained 4.9 and 4.5 min for the coastal seawater DOM and Suwannee River NOM fractions, respectively, with fraction 4 retained 5.30 and 5.20 min, fraction 5 retained 5.55 and 5.50 min, fraction 6 retained 6.25 and 6.10 min, fraction 7 retained 7.0 and 6.9 min, and fraction 8 retained 7.8 and 7.9 min, respectively. These variations in retention times, although small, are greater than that seen for single standards and again reflect differences in the exact isomeric content of the two sets of fractions.

The significance of these overlaid chromatograms lies within the overall resolution possible through the combined monolithic column fractionation, and subsequent RP-HPLC/HR-MS separation and detection. Similar resolution of specific groups of isomers could be seen across the mass spectrum for each sample. The chromatograms shown in Fig. 9 certainly represent some of the most highly resolved separations achieved to-date for these complex DOM and NOM mixtures, and provide a basis for much greater examination and investigation of the complex isomeric nature of CRAM and CRAM-like material. Clearly these resolved peaks on the second dimension separation would point to the presence of possibly dozens of isomers for each of the many hundreds of ions identified by HRMS.

## Conclusions

A two-dimensional reversed-phase chromatographic approach to the fractionation and separation of DOM and NOM has been developed. A high-capacity 1.1 m long reversed-phase monolithic column was applied to fractionate the DOM and NOM, prior to further fractional separation using standard RP-HPLC coupled with HRMS. These combined separation steps resulted in unprecedented resolution of isomeric material, typically present within CRAM and CRAM-like substances. Composite peaks observed in the second dimension separation of each collected fraction were subjected to HRMS analysis and characterisation using Van Krevelen diagrams, which revealed decreasing O/C ratios from earlier to later eluted fractions, and an increasing H/C ratio, indicative of an increasing degree of saturation. Plotting the weighted mean  $m/z$  for all ions observed in the composite peaks also revealed a very clear correlation between  $m/z$  and retention on the monolithic column, although interestingly the slopes from such plots for data recorded for a coastal seawater DOM and the Suwannee River reference material differed, providing an early indication of differences in the composition of the two samples. These differences were highlighted on closer inspection of the entire MS datasets for each fraction, namely a broader molecular weight distribution, and a higher degree of unsaturation in the case of Suwannee River NOM. However, such differences can be related to the extraction technique used to isolate the sample, and obviously the source of the sample, with freshwater DOM samples commonly characterised by a higher degree of unsaturation [43].

**Acknowledgements** This research was supported under Australian Research Council's Discovery Projects funding scheme (Project Number DP130101518).

## Compliance with Ethical Standards

**Conflict of interest** The authors declare no conflict of interest.

**Ethical approval** This article does not contain any studies with human participants or animals performed by any of the authors.

## References

1. Jiao N, Azam F, Sanders S (eds) (2011) Microbial carbon pump in the ocean. Science, AAAS Custom Publishing
2. Amon RMW, Benner R (1994) Nature 369:549
3. Hansell DA, Carlson CA (eds) (2014) Biogeochemistry of marine dissolved organic matter. 2nd edn. Academic press, London
4. Mopper K, Zhou X, Kieber RJ, Kieber DJ, Sikorski RJ, Jones RD (1991) Nature 353:60

5. Dalzell BJ, Minor EC, Mopper KM (2009) *Org Geochem* 40:243
6. Nawrocki MP, Karl DM (1989) *Mar Ecol Prog Ser* 57:35
7. Green NW, Perdue EM, Aiken GR, Butler KD, Chen H, Dittmar T, Niggemann J, Stubbins A (2014) *Mar Chem* 161:14
8. Perminova IV, Dubinenkov IV, Kononikhin AS, Konstantinov AI, Zhrebker AY, Andzhushev MM, Lebedev VA, Bulygina E, Holmes RM, Kostyukevich YI (2014) *Environ Sci Technol* 48:7461
9. Medeiros PM, Simoneit BR (2007) *J Chromatogr A* 1141:271
10. Louchouart P, Amon RMW, Duan S, Pondell C, Seward SM, White N (2010) *Mar Chem* 118:85
11. Lang SQ, Bernasconi SM, Früh-Green GL (2012) *Rapid Commun Mass Spectrom* 26:9
12. Parlanti E, Morin B, Vacher L (2002) *Org Geochem* 33:221
13. Dittmar T, Whitehead K, Minor EC, Koch BP (2007) *Mar Chem* 107:378
14. Koch BP, Ludwischowski K-U, Kattner G, Dittmar T, Witt M (2008) *Mar Chem* 111:233
15. Lang SQ, Bernasconi SM, Früh-Green GL (2012) *Rapid Commun Mass Spectrom* 26:9
16. Hertkorn N, Benner R, Frommberger M, Schmittkopplin P, Witt M, Kaiser K, Ketrup A, Hedges J (2006) *Geochim Cosmochim Acta* 70:2990
17. Gwen MJS, Woods C, Simpson AJ (2012) *Water Res* 46:3398
18. Lam B, Baer A, Alaei M, Lefebvre B, Moser A, Williams A, Simpson AJ (2007) *Environ Sci Technol* 41:8240
19. Stenson AC, Ruddy BM, Bythell BJ (2014) *Int J Mass Spectrom* 360:45
20. Capley EN, Tipton JD, Marshall AG, Stenson AC (2010) *Anal Chem* 82:8194
21. Stenson AC, Marshall AG, Cooper WT (2003) *Anal Chem* 75:1275
22. Woods GC, Simpson MJ, Simpson AJ (2012) *Water Res* 46:3398
23. Woods GC, Simpson MJ, Koerner PJ, Napoli A, Simpson AJ (2011) *Environ Sci Technol* 45:3880
24. Everett CR, Chin Y-P, Aiken G (1999) *Limnol Oceanogr* 44:1316
25. Minor EC, Simjouw JP, Boon JJ, Kerkhoff AE, van der Horst J (2002) *Mar Chem* 78:75
26. Her N, Amy G, McKnight D, Sohn J, Yoon Y (2003) *Water Res* 37:4295
27. Panagiotopoulos C, Repeta DJ, Johnson CG (2007) *Org Geochem* 38:884
28. Kaiser K, Benner R (2009) *Mar Chem* 113:63
29. Simpson TL, Simpson AJ, Spraul MJ, Braumann M, Kingery U, Kelleher WL, Kelleher BP, Hayes MH (2004) *Analyst* 129:1216
30. Mills GL, Quinn JG (1981) *Mar Chem* 10:93
31. Mills GL, McFadden E, Quinn JG (1987) *Mar Chem* 20:313
32. Liu Z, Sleighter RL, Zhong J, Hatcher PG (2011) *Est Coast Shelf Sci* 92:205
33. Bones J, Duffy C, Macka M, Paull B (2008) *Analyst* 133:180
34. Averett R, Leenheer J, McKnight D, Thorn K (1989) *US Geological survey open file report* 87
35. Serkiz SM, Perdue EM (1990) *Water Res* 24:911
36. Sun L, Perdue EM, McCarthy JF (1995) *Water Res* 29:1471
37. Thorsten Dittmar BK, Hertkorn N, Kattner G (2008) *Limnol Oceanogr Methods* 6:230
38. Wilde FD, Radtke DB, Gibs J, Iwatsubo RT (1998) *Techniques of water-resources investigations*, book 9, Geological Survey publication, US
39. Sandron S, Rojas A, Wilson R, Davies NW, Haddad P, Shellie R, Nesterenko PN, Kelleher B (2015) *B Paull Environ Sci Process Impacts* 17:1531
40. Sandron S, Nesterenko PN, McCaul MV, Kelleher B, Paull B (2014) *J Sep Sci* 37:135
41. Scott RPW (2003) *Preparative chromatography*, book 12, Chrom-Ed Book Series. [http://www.chromatography-online.org/books/preparative\\_chromatography/cc241/index.php](http://www.chromatography-online.org/books/preparative_chromatography/cc241/index.php). Accessed 17 May 2017
42. Tivendale ND, Davies NW, Horne J, Ross JJ, Smith JA (2015) *Aust J Chem* 68:345
43. Koprivnjak JF, Pfromm PH, Ingall E, Vetter TA, Schmitt-Kopplin P, Hertkorn N, Frommberger M, Knicker H, Perdue EM (2009) *Geochim et Cosmochim Acta* 73:4215
44. Vetter T, Perdue E, Ingall E, Koprivnjak J, Pfromm P (2007) *Sep Purif Technol* 56:383
45. Koprivnjak JF, Perdue EM, Pfromm PH (2006) *Water Res* 40:3385
46. Tfaily MM, Hodgkins S, Podgorski DC, Chanton JP, Cooper WT (2012) *Anal Bioanal Chem* 404:447
47. Davies NW, Sandron S, Nesterenko PN, Paull B, Wilson R, Haddad P, Shellie R, Rojas A (2015) *Environ Sci Process Impacts* 17:495
48. Kim S, Kramer RW, Hatcher PG (2003) *Anal Chem* 75:5336
49. Koch B, Witt M, Engbrodt R, Dittmar T, Kattner G (2005) *Geochim Cosmochim Acta* 69:3299
50. Alexandra AGM, Stenson C, William T (2003) *Cooper. Anal Chem* 75:1275
51. Stenson AC (2008) *Environ Sci Technol* 42:2060
52. Hertkorn N, Harir M, Koch B, Michalke B, Schmitt-Kopplin P (2013) *Biogeosciences* 10:1583